How Important is Working with an Ordered Electrode to Improve the Charge Collection Efficiency in Nanostructured Solar Cells?

ARTICLE *in* JOURNAL OF PHYSICAL CHEMISTRY LETTERS · JANUARY 2012

Impact Factor: 7.46 · DOI: 10.1021/jz2015988

3 AUTHORS, INCLUDING:

José Pablo González Vázquez
Universidad Pablo de Olavide
8 PUBLICATIONS **139** CITATIONS
SEE PROFILE

Juan A Anta
Universidad Pablo de Olavide
109 PUBLICATIONS **1,800** CITATIONS
SEE PROFILE

THE JOURNAL OF PHYSICAL CHEMISTRY Letters

Letter

pubs.acs.org/JPCL

How Important is Working with an Ordered Electrode to Improve the Charge Collection Efficiency in Nanostructured Solar Cells?

J. P. Gonzalez-Vazquez,[†] Victor Morales-Flórez,[‡] and Juan A. Anta*[,†]

[†]Área de Química Física, Universidad Pablo de Olavide, Sevilla, Spain

[‡]Instituto de Ciencia de Materiales de Sevilla, CSIC-Universidad de Sevilla, Av. Américo Vespucio 49, E-41092 Sevilla, Spain

Supporting Information

ABSTRACT: The collection efficiency of carriers in solar cells based on nanostructured electrodes is determined for different degrees or morphological one-dimensional order. The transport process is modeled by random walk numerical simulation in a mesoporous electrode that resembles the morphology of nanostructured TiO_2 electrodes typically used in dye-sensitized solar cells and related systems. By applying an energy relaxation procedure in the presence of an external potential, a preferential direction is induced in the system. It is found that the partially ordered electrode can almost double the collection efficiency with respect to the disordered electrode. However, this improvement depends strongly on the probability of recombination. For too rapid or too slow recombination, working with partially ordered electrodes will not be beneficial. The computational method utilized here makes it possible to relate the charge collection efficiency with morphology. The collection efficiency is found to reach very rapidly a saturation value, meaning that, in the region of interest, a slight degree of ordering might be sufficient to induce a large improvement in collection efficiency.

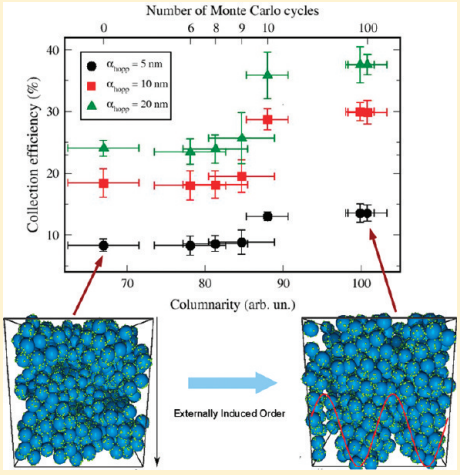

SECTION: Energy Conversion and Storage

New concepts in photovoltaics such as dye-sensitized solar cells,[1−3] organic solar cells,[4−6] hybrid solar cells,[7,8] and extremely thin absorber solar cells[9−11] are nowadays a primary topic of active research within the current quest for new sources of renewable energy. These emerging technologies attract interest due to the possibility of fabricating low-cost devices or developing applications where frontal and strong illumination is not required for good performance. These appealing properties rely on the nature of the materials utilized in their fabrication, nanostructured semiconductors (oxides and other inorganic combinations) and polymers. The fact that these materials are utilized in a disordered phase (although nanocrystalline in certain cases) makes unnecessary the highly expensive purification and crystallization process characteristic of high-performance solar cells. Furthermore, they allow for transparency, multiangle light harvesting, flexibility, and so forth.[12−16]

However, recently, there is renewed interest in improving the efficiency of these devices by working with one-dimensional (1D) ordered nanostructures such as nanowires, nanotubes, and so forth.[17−21] The idea is to improve the collection of charges using a photoanode where there is a more direct path toward the external circuit. This way, faster transport and slower recombination are theoretically achieved, so that charge and energy losses are minimized. Nevertheless, these structures are commonly difficult to prepare with the quality required for making efficient devices. Hence, the use of 1D nanostructures leads to the following paradox; the advantages of using a disordered material is sacrificed for the sake of improving the efficiency of the device. This paradox raises the question of the importance of the benefit of using 1D nanostructures.

In a previous report by Tirosh et al.,[22] the issue of the influence of the ordering of an anatase nanocrystalline structure on electron diffusion was studied. These authors found a substantial increase in the electron diffusion coefficient when a *partial* ordering is induced in the nanocrystalline electrode by means of an electric field that is applied during the deposition procedure. This enhancement was interpreted in terms of percolation effects. The influence of the percolation path in TiO_2 nanocomposites (considered via a variable porosity) has also been studied by Dittrich et al.[23] and Ofir et al.[24] These effects have also been described successfully by numerical modeling (random walk techniques).[25−28] The effect of morphology on charge transport has also been studied for many other systems.[29−31] However, the effect of the ordering with the consideration of both transport and recombination, which are crucial to understand the performance of nanostructured solar cells, remains to be comprehensively studied. In this regard, it has been pointed out recently[32] that the

Received: December 5, 2011
Accepted: January 15, 2012

   dx.doi.org/10.1021/jz2015988 | *J. Phys. Chem.Lett.* 2012, 3, 386−393

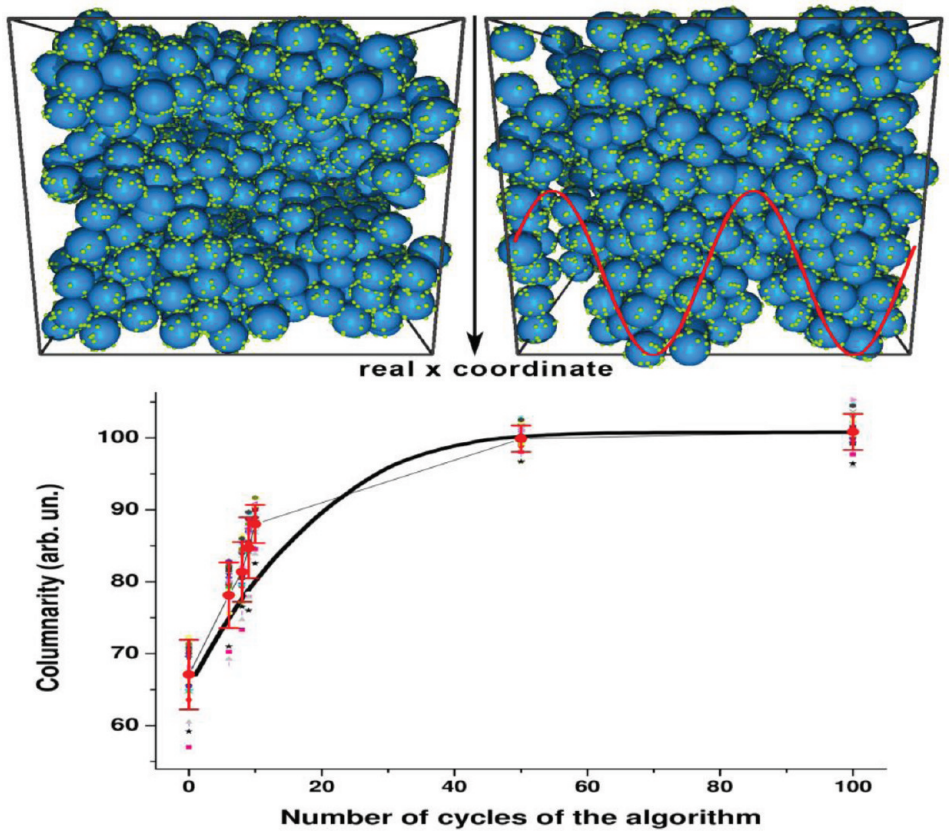

Figure 1. (Top left) Simulation box (size ≈ 400 nm) with a random packing of nanospheres with electron traps located on the surface (R^2 model). (Top right) Same as the left but with a partial order induced along the *x*-direction by MC energy minimization. The external periodic potential is plotted with a red solid line. (Bottom) Columnarity of the array of nanospheres (symbols) for various replicas and energy difference with respect to the minimum (solid line) versus the number of cycles executed in the minimization procedure. Energy variation is normalized with respect to the starting situation, $1-(E - E_{min})/(E_{max} - E_{min})$ and scaled for comparison purposes.

alleged benefit of using 1D nanostructures should be taken with reserve, especially for DSC architectures where charge collection already approaches 100%.

In this work, we address this issue by exploring the relationship between the degree of order and the charge collection efficiency. The main objective is to find a semiquantitative functional relation between the increase in efficiency and an appropriate order parameter. This functional relation will help to assess the improvement produced by a hypothetical ordering of a disordered nanostructure substrate typically used in dye-sensitized solar cells.[33] This problem is addressed from the theoretical point of view using numerical methods.[34,35] The advantage of using numerical simulation is that the degree of order and the charge collection efficiency can be more easily and unambiguously measured, isolating the effect of the order from other effects such as the specific surface or the recombination rate. For instance, very recently,[36] ab initio simulation has proven very useful to describe non-adiabatic charge transfer from quantum dots to the TiO_2 surface. In this work, we study the effect of order on charge transfer, including transport and recombination, but on a larger spatial scale, not accessible to ab initio methods. As in this and previous theoretical works, the aim is to clarify and help guide future research, which should be focused on obtaining better-functioning devices by addressing the key issues that limit efficiency.[32]

The charge collection efficiency in photoelectrochemical cells is defined as the ratio between the number of charge carriers (electrons or holes) collected in the external circuit and the number of photogenerated carriers. This can be expressed as[3]

$$\eta_{col} = \frac{\tau_{rec}}{\tau_{rec} + \tau_{tr}} \quad (1)$$

where τ_{rec} and τ_{tr} are the lifetime and the transport time of charge carriers, respectively (measured at coincident positions of the Fermi level). The collection efficiency has typically been discussed in the current literature in terms of the diffusion length,[37−40] which represents the average distance that carriers can travel in the material. For the case of linear recombination kinetics,[38] this is shown to be equal to

$$L = (D\tau_{rec})^{1/2} \quad (2)$$

where *D* is the diffusion coefficient. (As discussed in detail in ref 38, if recombination is not linear, eq 2 is used to define a "small perturbation" diffusion length, which is still useful to diagnose the collection efficiency of the device.) Hence, the longer the *L*, the larger the probability of collecting charges in the external contact. Both eqs 1 and 2 show that good collection efficiency arises from a balance of fast transport and slow recombination. The effect produced by the use of 1D nanostructures is either to accelerate transport or to minimize recombination (or both).

The random walk numerical simulation (RWNS) method[34,41] is a stochastic calculation that makes it possible to obtain dynamic properties in disordered media starting from a

dx.doi.org/10.1021/jz2015988 | J. Phys. Chem.Lett. 2012, 3, 386−393

simple model of transport and recombination in the material. In a RW simulation, a number of carriers are allowed to move randomly in a three-dimensional network of sites. According to a specific transport model (either multiple trapping[42−44] or hopping[45−47]), each site in the network is given a certain release or "detrapping" time that determines the probability (i.e., the hopping rate) for a carrier to jump to another site. In a previous work,[28] we utilized this method to study electron transport in a realistic random packing of nanospheres. The method allowed us to establish how the diffusion coefficient depends on the porosity of the material and on the size of the nanospheres. In this calculation, electron traps were placed either on the surface of the nanosphere (R^2 model) or in the bulk (R^3 model). The comparison with experiment showed that the R^2 model is more realistic. This is justified by the fact that carrier traps are most likely located on the surface of nanocrystallites as it is there where point defects appear and where the interaction with ions of opposite charge takes place. More recently,[39] we introduced recombination in the numerical procedure so that the lifetime and the diffusion length of electrons can be measured by averaging over trajectories generated stochastically. The method provides data for the voltage dependence of the diffusion length upon Fermi level variations.

With the aim of studying the effect of working with a 1D nanostructure, in this work, we introduce order in a random packing of nanospheres (see Figure 1), which simulates realistic disordered porous TiO_2 nanostructures. To do so, we start from a random hierarchical packing generated by means of the cluster model.[35] In this calculation, a nanosphere radius of 20 nm has been considered, and a low overlapping between neighboring nanospheres has been imposed, which was kept constant along all of the simulated structures. Given the statistical uncertainty implicit to the construction algorithm, we have worked with five different statistically independent replicas, and averages were extracted. All of them comply with the following morphological parameters: specific surface area, $S = 27.0 \pm 0.8$ m^2/g; porosity, $P = 56 \pm 3\%$; and density, $\rho = 1.7 \pm 0.1$ g/cm^3. To induce an ordering effect, these random structures were then exposed to an external 2D sinusoidal potential parallel to the collecting substrate (see Figure 1). The sine function is especially adequate in this context as it is a continuous, analytic, and periodic potential. By minimizing the potential energy of the system using the Monte Carlo (MC) technique,[48] 1D order is progressively induced in the system. This is achieved by running a specific number of MC cycles and without altering significantly the morphological parameters indicated above (see Supporting Information for details). This way, different particulate realistic nanostructures are built without changing no other structural parameters than 1D order. Finally, following previous work,[28,49,50] we place "electron" traps on the surface of the nanospheres (R^2 model). For each of the five replicas, a minimum of 25 different sets of traps were placed and considered for the RW simulations described below.

The spatial location of the electron traps makes it possible to measure the 1D order of the system with respect to the direction perpendicular to the collecting substrate (x). To do so, we use an order parameter based on a concept of "columnarity". This is estimated by computing the standard deviation of a distribution of the trap coordinates with respect to their projected positions on a grid located on the plane parallel to the collecting substrate, that is, perpendicular to the preferred columnar direction (see Supporting Information for further details). Hence, a larger columnar order implies a wider distribution, with a larger standard deviation, as traps tend to accumulate at specific positions in the grid.

Figure 1 shows how the columnarity and the total energy vary with respect to the number of iterations or cycles employed in the Monte Carlo energy minimization procedure. To estimate the statistical uncertainty of the packing algorithm, results for the five replicas of the packing of nanospheres are presented. (For each replica, the ordering process of energy minimization is applied.) Note that full minimization (meaning an equilibrated situation) does not imply that perfect crystalline order is achieved but that just a preferential direction is induced in the system along the x-direction. It is observed that there is a direct correspondence between the relative columnarity parameter and the relaxation energy. The main conclusion is that the extent of the minimization procedure (i.e., the number of MC cycles) can be used to *tune* the degree of order in the system, hence allowing for a systematic investigation of the effect on the charge collection efficiency in the presence of a preferential direction in the nanostructured electrode.

The placement of electron traps on the surface of the nanospheres and the ordering procedure described above provide a three-dimensional network of sites as input for a RWNS calculation.[28,34,39,41,46,51] The simulation was performed using Miller−Abrahams hopping rates.[52] This means that hopping times for carriers moving between neighboring traps are computed via

$$t_{ij} = -\ln(R)t_0 \exp\left[2\frac{r_{ij}}{\alpha_{\text{hopp}}} + \frac{E_j - E_i}{2k_BT} + \frac{|E_j - E_i|}{2k_BT}\right] \quad (3)$$

where R is a random number distributed uniformly between 0 and 1, t_0 is the inverse of the attempt-to-jump frequency, r_{ij} is the distance between the traps, α_{hopp} is the localization radius for hopping, and E_j and E_i are the energies of the target and starting traps, respectively. These energies are extracted from an exponential distribution[53]

$$g(E) = \frac{N_L}{k_BT_0} \exp[(E - E_c)/k_BT_0] \quad (4)$$

where N_L is the total trap density, T_0 is the characteristic temperature of the distribution, and E_c is the energy of the conduction band or mobility edge. Note that $E - E_c$ is always negative and becomes more negative as one moves deeper in the conduction band. By means of eqs 3 and 4, spatial and energy disorder are adequately taken into account in the transport process for a combination of parameters. In this work, we used[53,54] $T_0 = 1100$ K, $T = 300$ K, and $t_0 = 10^{-12}$ s. A surface trap density of 0.004 nm^{-2} (with respect to the nanosphere surface) was considered.[28] This corresponds to a volumetric trap density of 2.3×10^{-4} nm^{-3} (meaning that traps are located at an average distance of 16 nm in the film). In connection to this, three localization radii of $\alpha_{\text{hopp}} = 2.5$, 10, and 20 nm have been studied. It is important to note that because the traps are located on the surface of the nanospheres and these are in contact, the actual distance between a particular trap and its neighbors is shorter, hence allowing for percolation of carriers throughout the network.

dx.doi.org/10.1021/jz2015988 | J. Phys. Chem.Lett. 2012, 3, 386−393

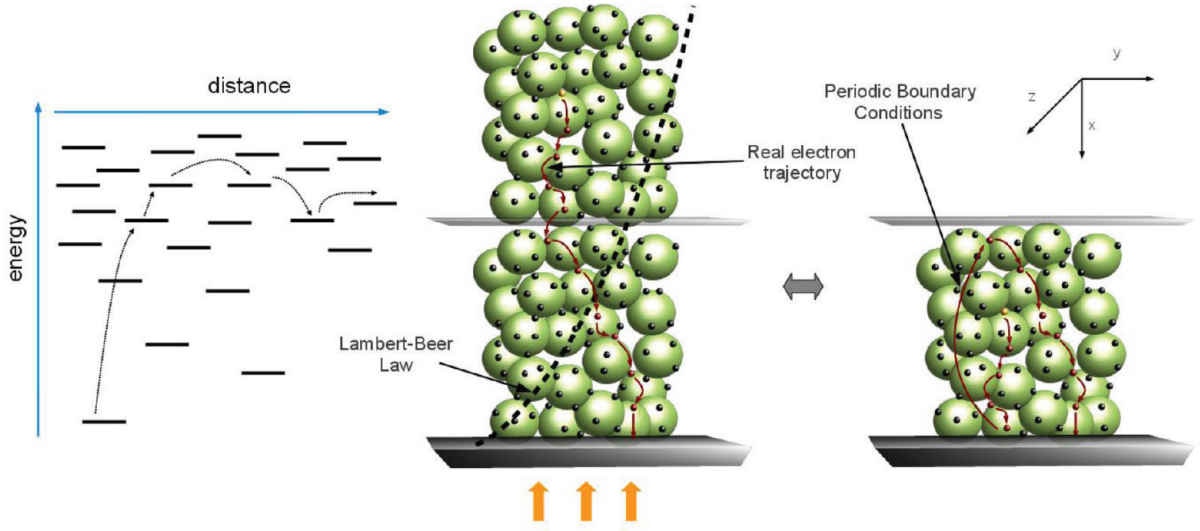

Figure 2. Illustration of the RWNS calculation utilized in this work. (Left) Hopping transport in an exponential distribution of trap energies. (Middle and right) Hopping transport in a packing of nanospheres, with the traps (black dots) located on their surface. The dashed line stands for the carrier generation profile, which resembles a Lambert−Beer law for light coming in the *x*-direction. The simulation box is periodically replicated in the three directions of space to simulate the hopping transport (right), but real coordinates are considered to describe injection and collection (middle).

An illustration of the hopping transport of electrons in an exponential distribution of localized states is presented in Figure 2. In addition to transport, also recombination should be considered to study charge collection efficiency. Following ref 39, we introduced a constant probability (independent of trap energy) for carrier removal. As shown in that work, this probability leads to an exponential distribution of survival times for carriers, which defines a carrier lifetime. This lifetime defines in turn the characteristic diffusion length of the system. In previous work,[39] this probability was adjusted to give diffusion lengths on the order of micrometers, leading to the general result that in typical DSCs, the time scale for recombination is much longer that the time scale for transport. In this work, we ran calculations analogous to those of ref 39 to determine the characteristic diffusion lengths of the practical cases for which the charge collection efficiency is calculated. Recombination probabilities ranged between $P_R = 10^{-10}$ and 10^{-2} in arbitrary units. As describe below, this is translated to a range of values for the diffusion length; the smaller the P_R, the longer the diffusion length.

The description of the solar cell at real working conditions implies the use of a considerable number of carriers and trap states, which leads to very high numerical demands. To reduce the computational time, the following approximations are implemented. On the one hand, the exponential distribution in eq 4 is truncated for energies below the Fermi level, hence assuming that deeper traps are always occupied. This is the so-called one-electron approximation that makes it possible to simulate transport at a given position of the Fermi level with the movement of a single carrier.[39,55] On the other hand, periodic boundary conditions are considered in the three directions of space.[48] Hence, the simulation box in Figure 1 is periodically replicated in such a way that if a carrier crosses one of the box boundaries, it is automatically reinjected through the opposite boundary.

In this work, we aim to calculate charge collection efficiency in realistic systems, and this requires consideration of charge generation in accordance with optical absorption lengths on the order of micrometers, typical of the dyes used in dye-sensitized solar cells and related devices (for instance, the extinction coefficient of typical ruthenium dyes[56] is 1.4×10^4 M^{-1} cm^{-1} at $\lambda \approx 520$ nm. For common dye loadings of $2-3 \times 10^{-7}$ mol/cm^2, one obtains absorption lengths of 2−4 μm). However, the use of a simulation box on the order of micrometers is not computationally feasible for the trap densities used here. To surmount this problem, we have devised a numerical procedure where the actual distance of the carrier with respect to the collecting substrate is continuously stored during the simulation. In practice, we carry out a typical simulation of an infinite system (with periodic boundary conditions). However, in addition, the actual *x*-position of the carrier is also taken into account. This is considered in two steps of the algorithm, (1) when carriers are injected in the sample along the *x*-direction according to the Lambert−Beer law (see Figure 2) and (2) when carriers are collected at $x = 0$. Therefore, the fictitious coordinates arising from the application of the periodic boundary conditions are only considered in eqs 3 and 4, but injection and collection are modeled according to a real coordinate. This way, a macroscopic film with a size of micrometers can be adequately simulated with a manageable number of nanospheres and traps.

The adequate implementation of this procedure is tested in Figure 3. In the simulation, carriers are injected along the *x*-axis according to a probability given by the Lambert−Beer law, $\exp(-x/L_{ab})$, where L_{ab} is the characteristic optical absorption length. This depends on the optical features of the solar cell (concentration and absorption coefficient of the absorbing material). Four cases have been considered for this parameter, ranging between $L_{ab} = 300$ and 3300 nm. In Figure 3, the charge collection efficiency is plotted versus L_{ab} and the Fermi level position. The simulation results demonstrate that collection increases when the absorption length is shorter. Therefore, as expected, collection is more efficient for highly absorbing materials because carriers are generated, on average, closer to the collecting electrode. The collection efficiency is found to depend on L_{ab} according to a power law. This behavior is found to be also predicted by the numerical solution of the continuity equation for electrons in the photoanode[57−59]

dx.doi.org/10.1021/jz2015988 | J. Phys. Chem.Lett. 2012, 3, 386−393

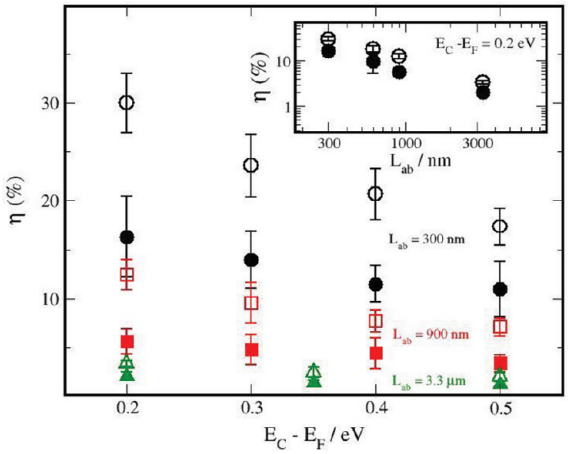

Figure 3. Charge collection efficiency as a function of Fermi level position for a random packing of nanospheres (solid symbols; see the top left panel in Figure 1) and a fully relaxed ordered structure (open symbols; see the top right panel in Figure 1) at different values of the absorption length L_{ab}. In the inset, the collection efficiency is plotted versus L_{ab} for $E_c - E_F = 0.2$ eV on a double logarithmic scale. Error bars are derived from results of statistically independent morphological replicas. Simulations were carried out for the following parameters: T_0 = 1100 K, T = 300 K, t_0 =10^{-12} s, surface trap density = 0.004 nm^{-2}, α_{hopp} = 2.5 nm, and nanosphere radius = 20 nm. $P_R = 10^{-6}$ arbitrary units.

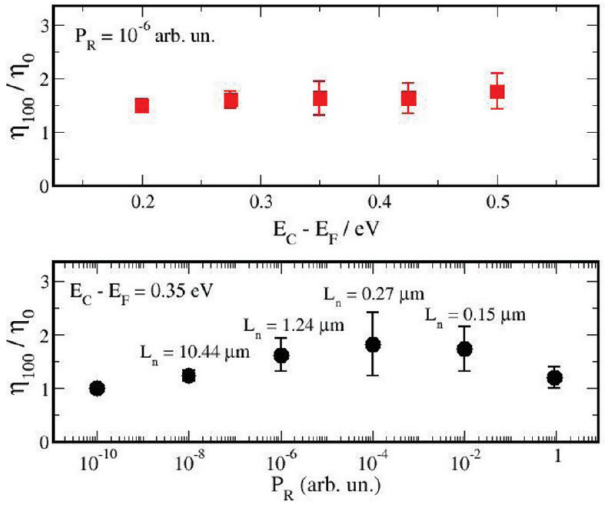

Figure 4. Charge collection efficiency improvement ratio for ordered structures (100 cycles; see Figure 1) with respect to a random packing of nanospheres. (Top panel) Improvement ratio versus Fermi level at a constant recombination probability. (Bottom panel) Improvement ratio versus recombination probability at a fixed Fermi level. The results for the diffusion length from simulations on an infinite fully disordered system[39] are indicated. Error bars are derived from results of statistically independent morphological replicas. Simulations were carried out for the following parameters: T_0 = 1100 K, T = 300 K, t_0 = 10^{-12} s, surface trap density = 0.004 nm^{-2}, α_{hopp} = 10 nm, nanosphere radius = 20 nm, and L_{ab} = 3.3 μm.

(see Supporting Information for details). The RW simulations give power law exponents of 0.7−0.8, whereas the numerical solution yields 0.65 for the equivalent case.

On the other hand, the collection efficiency decreases as the Fermi level gets deeper into the conduction band. This behavior is only clearly observed for short absorption lengths. For longer absorption lengths, the effect of the Fermi level is marginal. This observation can be interpreted in terms of the Fermi-level dependence of the diffusion coefficient.[46,55] If E_F is raised, carriers diffuse more rapidly, and the collection efficiency is increased. However, for long optical lengths, carriers are generated at further distances, and the probability of recombining before being collected becomes more important. Therefore, the effect of a more rapid transport in minimized.

The influence of morphological (1D) order on charge collection efficiency is reported in Figure 4 for different positions of the Fermi level and different recombination probabilities. In Figure 4, the collection efficiency for the structure with the maximum degree of ordering (100 cycles in Figure 1) is compared to that of the disordered structure using the ratio η_{100}/η. The results of the simulations demonstrate that the collection efficiency can be improved by a factor close to 2 when a preferential direction is introduced in the system. This improvement is found to be roughly independent of the Fermi level (Figure 4, upper panel), suggesting that either the illumination intensity or applied voltage would not modify this morphological effect.

As could be expected, the enhancement in collection efficiency is found to depend strongly on the kinetics of carrier recombination, that is, on the carrier lifetime. In the lower panel of Figure 4, the improvement factor is plotted against the recombination probability P_R. For very slow recombination, corresponding to very long diffusion lengths, the effect of the ordering is absent because the collection efficiency approaches 100% in both cases. This means that there is no benefit in providing a more direct percolation path to the external contact if the lifetime of the electrons is long enough. The opposite situation corresponds to very rapid recombination, with short diffusion lengths. In that case, no benefit is observed either because the average distance traveled by the carriers is much smaller than the characteristic length scale of the columnar order imposed in the system. As a rule of thumb, it could be stated that the "ordering" effect is only observed when the diffusion length L_n is approximately of the same order of magnitude as the optical absorption length L_{ab} and the characteristic length scale in which the order is induced. As can be seen in the lower panel of Figure 4, maximum efficiencies are obtained for recombination probabilities of P_R = 10^{-5}−10^{-3} arbitrary units. Simulations in an infinite system for a random packing give an average[39] of $L_n \approx 1.0$−0.2 μm for these probabilities, whereas the value used for the absorption length was L_{ab} = 3.3 μm.

The possibility of tuning the degree of 1D order by a partial run of the energy minimization algorithm permits us to investigate whether an approximate functional relationship can be found between the collection efficiency and the order parameter (columnarity). Results for this are presented in Figure 5, where we have chosen an intermediate value of the recombination probability to better see the effect of the ordering. In this figure, the collection efficiency extracted from the RWNS calculations is plotted against the columnarity. The RWNS results confirm the progressive enhancement in collection efficiency when the order of the structure is increased. However, it is noteworthy that this enhancement does not occur linearly. The numerical data show that the improvement is significant even for a weak ordering of the system, with a sudden increase at intermediate values of the columnarity (~86, 9−10 cycles). Thus, the collection efficiency reaches rapidly a saturation value, resembling a sigmoidal function. It must be recalled that even for the situation with

dx.doi.org/10.1021/jz2015988 | J. Phys. Chem.Lett. 2012, 3, 386−393

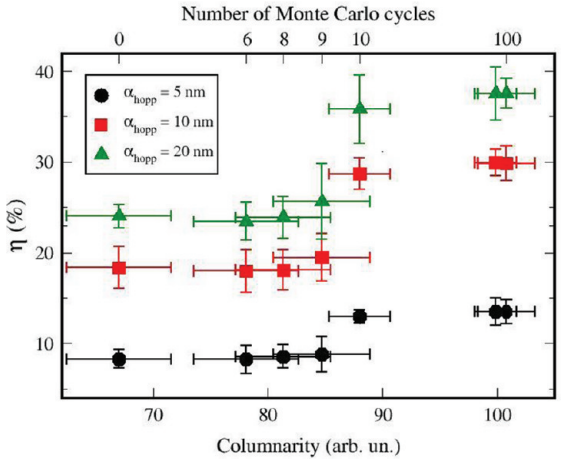

Figure 5. Carrier collection efficiency as a function of the columnarity as extracted from RWNS calculations for different localization radii for an intermediate value of the recombination probability $P_R = 10^{-6}$ arbitrary units. Error bars are derived from results of statistically independent morphological replicas. Simulations were carried out for the following parameters: T_0 = 1100 K, T = 300 K, $t_0 = 10^{-12}$ s, surface trap density = 0.004 nm^{-2}, nanosphere radius = 20 nm, and $E_c - E_F$ = 0.35 eV. Note that a longer localization radius lead to better efficiencies as carriers travel longer distances between recombination events.

maximum columnarity (full energy minimization, 100 cycles), the system does not have perfect crystalline order. In fact, it is basically a disordered structure but with a preferential alignment along the *x*-direction induced by the external potential. The present results suggest that the introduction of a very slight degree of order in the nanostructure can lead to a huge and abrupt increase in collection efficiency.

The reason for the abrupt jump in the collection efficiency at intermediate order seems to be related to the existence of a percolation "threshold" in the plane perpendicular to the columnar direction. The relevance of the connectivity of the transport sites in the adequate direction has been stressed by several authors.[26,30,60] In this case, we have an effect of improved connectivity, but only in one direction. This acts in the following manner: when a columnar order is induced, gaps with very low trap density are created between the columns. This hinders the perpendicular jumping of the carriers and favors their harvesting in the collecting substrate. This hypothesis can be inferred from the "softening" of the jump when longer localization radii (meaning longer diffusion lengths) are utilized in the simulation. Hence, when electrons travel shorter distances, they find it more difficult to percolate in directions parallel to the collecting surface when the systems are "more columnar". However, further work is required to elucidate the precise origin of this behavior and the actual relationship between morphological order and transport properties in disordered semiconductors.

In summary, we have developed a numerical procedure that permits one to obtain the collection efficiency of photogenerated charges in nanostructured electrodes with different degrees of 1D order. The simulated system resembles a real nanostructure where charges are generated according to a Lambert–Beer law with the optical length of the order of micrometers and where transport and recombination are taken into account via a hopping model coupled with a constant recombination probability. The results show that the collection efficiency would be almost doubled by a partial ordering of the system. The maximum efficiency enhancement only takes place if the recombination probability (which determines the characteristic diffusion length of the system) is not too rapid or too low, with a diffusion length of the same order of magnitude as the optical absorption length. Furthermore, the collection efficiency can be calculated as a function of the degree of order via a normalized order parameter. The results show that a very slight degree of 1D order can lead to a significant increase of the collection efficiency. The predictions contained in this theoretical work might be interesting to develop strategies where a preferential direction is induced in an originally disordered structure, such as in the use of hierarchical structures studied in the recent literature.

■ ASSOCIATED CONTENT

Supporting Information

Ordering algorithm and columnarity measurements. Theoretical dependence of the collection efficiency on the absorption length. This material is available free of charge via the Internet at http://pubs.acs.org.

■ ACKNOWLEDGMENTS

We thank the *Ministerio de Ciencia e Innovación* of Spain for funding under Project HOPE CSD2007-00007 (Consolider-Ingenio 2010) and CTQ2009-10477 and Junta de Andalucía under Projects P06-FQM-01869, P07-FQM-02595, and P07-FQM-02600. V.M.F. thanks the CSIC for financial support through the JAE program. We also thank S. Dominguez-Meister, from the ICMS, for the development of the "Dmeister algorithm" to quantify the degree of 1D order for columnar systems.

■ REFERENCES

(1) O'Regan, B.; Gratzel, M. A Low-Cost, High-Efficiency Solar-Cell Based on Dye-Sensitized Colloidal TiO_2 Films. *Nature* **1991**, *353*, 737–740.

(2) Grätzel, M. Recent Advances in Sensitized Mesoscopic Solar Cells. *Acc. Chem. Res.* **2009**, *42*, 1788–1798.

(3) Hagfeldt, A.; Boschloo, G.; Sun, L.; Kloo, L.; Pettersson, H. Dye-Sensitized Solar Cells. *Chem. Rev.* **2010**, *110*, 6595–6663.

(4) Brabec, C. J.; Sariciftci, N. S.; Hummelen, J. C. Plastic Solar Cells. *Adv. Funct. Mater.* **2001**, *11*, 15–26.

(5) Campoy-Quiles, M.; Ferenczi, T.; Agostinelli, T.; Etchegoin, P. G.; Kim, Y.; Anthopoulos, T. D.; Stavrinou, P. N.; Bradley, D. D. C.; Nelson, J. Morphology Evolution via Self-Organization and Lateral and Vertical Diffusion in Polymer: Fullerene Solar Cell Blends. *Nat. Mater.* **2008**, *7*, 158–164.

(6) Forrest, S. R. The Path to Ubiquitous and Low-Cost Organic Electronic Appliances on Plastic. *Nature* **2004**, *428*, 911–918.

(7) Yoshida, T.; Zhang, J. B.; Komatsu, D.; Sawatani, S.; Minoura, H.; Pauporte, T.; Lincot, D.; Oekermann, T.; Schlettwein, D.; Tada, H.; Wohrle, D.; Funabiki, K.; Matsui, M.; Miura, H.; Yanagi, H. Electrodeposition of Inorganic/Organic Hybrid Thin Films. *Adv. Funct. Mater.* **2009**, *19*, 17–43.

(8) Bandara, J.; Willinger, K.; Thelakkat, M. Multichromophore Light Harvesting in Hybrid Solar Cells. *Phys. Chem. Chem. Phys.* **2011**, *13*, 12906–12911.

(9) Kieven, D.; Dittrich, T.; Belaidi, A.; Tornow, J.; Schwarzburg, K.; Allsop, N.; Lux-Steiner, M. Effect of Internal Surface Area on the Performance of $ZnO/In_2S_3/CuSCN$ Solar Cells with Extremely Thin Absorber. *Appl. Phys. Lett.* **2008**, *92*, 153107.

(10) Dittrich, T.; Kieven, D.; Belaidi, A.; Rusu, M.; Tornow, J.; Schwarzburg, K.; Lux-Steiner, M. C. Formation of the Charge Selective

Contact in Solar Cells with Extremely Thin Absorber based on ZnO-Nanorod/In_2S_3/CuSCN. *J. Appl. Phys.* **2009**, *105*, 034509.
(11) Ernst, K.; Belaidi, A.; Konenkamp, R. Solar Cell with Extremely Thin Absorber on Highly Structured Substrate. *Semicond. Sci. Technol.* **2003**, *18*, 475−479.
(12) Gratzel, M. Photoelectrochemical Cells. *Nature* **2001**, *414*, 338−344.
(13) Yoon, S.; Tak, S.; Kim, J.; Jun, Y.; Kang, K.; Park, J. Application of Transparent Dye-Sensitized Solar Cells to Building Integrated Photovoltaic Systems. *Building and Environment* **2011**, *46*, 1899−1904.
(14) Fung, T. Y. Y.; Yang, H. Study on Thermal Performance of Semi-Transparent Building-Integrated Photovoltaic Glazings. *Energy and Buildings* **2008**, *40*, 341−350.
(15) Toyoda, T. Outdoor Performance of Large Scale Dsc Modules. *J. Photochem. Photobiol., A* **2004**, *164*, 203−207.
(16) Dennler, G.; Forberich, K.; Scharber, M. C.; Brabec, C. J.; Tomiš, I.; Hingerl, K.; Fromherz, T. Angle Dependence of External and Internal Quantum Efficiencies in Bulk-Heterojunction Organic Solar Cells. *J. Appl. Phys.* **2007**, *102*, 054516.
(17) Law, M.; Greene, L. E.; Johnson, J. C.; Saykally, R.; Yang, P. Nanowire Dye-Sensitized Solar Cells. *Nat. Mater.* **2005**, *4*, 455−459.
(18) Galoppini, E.; Rochford, J.; Chen, H. H.; Saraf, G.; Lu, Y. C.; Hagfeldt, A.; Boschloo, G. Fast Electron Transport in Metal Organic Vapor Deposition Grown Dye-Sensitized ZnO Nanorod Solar Cells. *J. Phys. Chem. B* **2006**, *110*, 16159−16161.
(19) Gonzalez-Valls, I.; Lira-Cantu, M. Vertically-Aligned Nanostructures of Zno for Excitonic Solar Cells: A Review. *Energy Environ. Sci.* **2009**, *2*, 19−34.
(20) Martinson, A. B. F.; McGarrah, J. E.; Parpia, M. O. K.; Hupp, J. T. Dynamics of Charge Transport and Recombination in ZnO Nanorod Array Dye-Sensitized Solar Cells. *Phys. Chem. Chem. Phys.* **2006**, *8*, 4655−4659.
(21) Liu, B.; Aydil, E. S. Growth of Oriented Single-Crystalline Rutile TiO_2 Nanorods on Transparent Conducting Substrates for Dye-Sensitized Solar Cells. *J. Am. Chem. Soc.* **2009**, *131*, 3985−3990.
(22) Tirosh, S.; Dittrich, T.; Ofir, A.; Grinis, L.; Zaban, A. Influence of Ordering in Porous TiO_2 Layers on Electron Diffusion. *J. Phys. Chem. B* **2006**, *110*, 16165−16168.
(23) Dittrich, T.; Ofir, A.; Tirosh, S.; Grinis, L.; Zaban, A. Influence of the Porosity on Diffusion and Lifetime in Porous TiO_2 Layers. *Appl. Phys. Lett.* **2006**, 88.
(24) Ofir, A.; Dor, S.; Grinis, L.; Zaban, A.; Dittrich, T.; Bisquert, J. Porosity Dependence of Electron Percolation in Manoporous TiO_2 Layers. *J. Chem. Phys.* **2008**, 128.
(25) Benkstein, K. D.; Kopidakis, N.; Lagemaat, J.; van de; Frank, A. J. Influence of the Percolation Network Geometry on Electron Transport in Dye-Sensitized Titanium Dioxide Solar Cells. *J. Phys. Chem. B* **2003**, *107*, 7759−7767.
(26) Cass, M. J.; Qiu, F. L.; Walker, A. B.; Fisher, A. C.; Peter, L. M. Influence of Grain Morphology on Electron Transport in Dye Sensitized Nanocrystalline Solar Cells. *J. Phys. Chem. B* **2003**, *107*, 113−119.
(27) Cass, M. J.; Walker, A. B.; Martinez, D.; Peter, L. M. Grain Morphology and Trapping Effects on Electron Transport in Dye-Sensitized Nanocrystalline Solar Cells. *J. Phys. Chem. B* **2005**, *109*, 5100−5107.
(28) Anta, J. A.; Morales-Florez, V. Combined Effect of Energetic and Spatial Disorder on the Trap-Limited Electron Diffusion Coefficient of Metal-Oxide Nanostructures. *J. Phys. Chem. C* **2008**, *112*, 10287−10293.
(29) Novak, S.; Hrach, R.; Svec, M. Relationship between Electrical and Morphological Properties of Nanocomposites. *Thin Solid Films* **2011**, *519*, 4012−4017.
(30) Vehoff, T.; Baumeier, B.; Troisi, A.; Andrienko, D. Charge Transport in Organic Crystals: Role of Disorder and Topological Connectivity. *J. Am. Chem. Soc.* **2010**, *132*, 11702−11708.
(31) Deng, H.; Zhang, R.; Bilotti, E.; Loos, J.; Peijs, T. Conductive Polymer Tape Containing Highly Oriented Carbon Nanofillers. *J. Appl. Polym. Sci.* **2009**, *113*, 742−751.
(32) Peter, L. M. The Grätzel Cell: Where Next? *J. Phys. Chem. Lett.* **2011**, *2*, 1861−1867.
(33) Oskam, G. Dye-Sensitized, Nanostructured Metal Oxide Photoelectrodes for Solar Energy Conversion. *Curr. Top. Electrochem.* **2004**, *10*, 141−162.
(34) Anta, J. A. Random Walk Numerical Simulation for Solar Cell Applications. *Energy Environ. Sci.* **2009**, *2*, 387−392.
(35) Morales-Florez, V.; Pinero, M.; Rosa-Fox, N. D. L.; Esquivias, L.; Anta, J. A. The Cluster Model: A Hierarchically-Ordered Assemblage or Random-Packing Spheres for Modelling Microstructures of Random Materials. *J. Non-Cryst. Solids* **2008**, *354*, 193−198.
(36) Long, R.; Prezhdo, O. V. Ab Initio Nonadiabatic Molecular Dynamics of the Ultrafast Electron Injection from a PbSe Quantum Dot into the TiO_2 Surface. *J. Am. Chem. Soc.* **2011**, *133*, 19240−19249.
(37) Peter, L. M. Characterization and Modeling of Dye-Sensitized Solar Cells. *J. Phys. Chem. C* **2007**, *111*, 6601−6612.
(38) Bisquert, J.; Mora-Seró, I. Simulation of Steady-State Characteristics of Dye-Sensitized Solar Cells and the Interpretation of the Diffusion Length. *J. Phys. Chem. Lett.* **2010**, *1*, 450−456.
(39) Gonzalez-Vazquez, J. P.; Anta, J. A.; Bisquert, J. Determination of the Electron Diffusion Length in Dye-Sensitized Solar Cells by Random Walk Simulation: Compensation Effects and Voltage Dependence. *J. Phys. Chem. C* **2010**, *114*, 8552−8558.
(40) Navas, J.; Guillén, E.; Alcántara, R.; Fernández-Lorenzo, C.; Martín-Calleja, J.; Oskam, G.; Idígoras, J.; Berger, T.; Anta, J. A. Direct Estimation of the Electron Diffusion Length in Dye-Sensitized Solar Cells. *J. Phys. Chem. Lett.* **2011**, *0*, 1045−1050.
(41) Nelson, J. Continuous-Time Random-Walk Model of Electron Transport in Nanocrystalline TiO_2 Electrodes. *Phys. Rev. B* **1999**, *59*, 15374−15380.
(42) Bisquert, J. Fractional Diffusion in the Multiple-Trapping Regime and Revision of the Equivalence with the Continuous-Time Random Walk. *Phys. Rev. Lett.* **2003**, 91.
(43) Vanmaekelbergh, D.; de Jongh, P. E. Electron Transport in Disordered Semiconductors Studied by a Small Harmonic Modulation of the Steady State. *Phys. Rev. B* **2000**, *61*, 4699.
(44) Tiedje, T.; Rose, A. A Physical Interpretation of Dispersive Transport in Disordered Semiconductors. *Solid State Commun.* **1981**, *37*, 49−52.
(45) Hartenstein, B.; Bässler, H. Transport Energy for Hopping in a Gaussian Density of States Distribution. *J. Non-Cryst. Solids* **1995**, *190*, 112−116.
(46) Gonzalez-Vazquez, J. P.; Anta, J. A.; Bisquert, J. Random Walk Numerical Simulation for Hopping Transport at Finite Carrier Concentrations: Diffusion Coefficient and Transport Energy Concept. *Phys. Chem. Chem. Phys.* **2009**, *11*, 10359−10367.
(47) Bisquert, J. Hopping Transport of Electrons in Dye-Sensitized Solar Cells. *J. Phys. Chem. C* **2007**, *111*, 17163−17168.
(48) Frenkel, D.; Smit, B. Understanding Molecular Simulation; Academic Press: New York, 2002.
(49) Kopidakis, N.; Neale, N. R.; Zhu, K.; Lagemaat, J.; van de; Frank, A. J. Spatial Location of Transport-Limiting Traps in TiO_2 Nanoparticle Films in Dye-Sensitized Solar Cells. *Appl. Phys. Lett.* **2005**, *87*, 202106.
(50) Zhu, K.; Kopidakis, N.; Neale, N. R.; Lagemaat, J.; van de; Frank, A. J. Influence of Surface Area on Charge Transport and Recombination in Dye-Sensitized TiO_2 Solar Cells. *J. Phys. Chem. B* **2006**, *110*, 25174−25180.
(51) Nelson, J.; Chandler, R. E. Random Walk Models of Charge Transfer and Transport in Dye Sensitized Systems. *Coord. Chem. Rev.* **2004**, *248*, 1181−1194.
(52) Miller, A.; Abrahams, E. Impurity Conduction at Low Concentrations. *Phys. Rev.* **1960**, *120*, 745−755.
(53) Bisquert, J.; Fabregat-Santiago, F.; Mora-Sero, I.; Garcia-Belmonte, G.; Barea, E. M.; Palomares, E. A Review of Recent Results on Electrochemical Determination of the Density of Electronic States of Nanostructured Metal-Oxide Semiconductors and Organic Hole Conductors. *Inorg. Chim. Acta* **2008**, *361*, 684−698.

(54) Anta, J. A.; Mora-Sero, I.; Dittrich, T.; Bisquert, J. Dynamics of Charge Separation and Trap-Limited Electron Transport in TiO_2 Nanostructures. *J. Phys. Chem. C* **2007**, *111*, 13997−14000.
(55) Anta, J. A.; Mora-Sero, I.; Dittrich, T.; Bisquert, J. Interpretation of Diffusion Coefficients in Nanostructured Materials from Random Walk Numerical Simulation. *Phys. Chem. Chem. Phys.* **2008**, *10*, 4478−4485.
(56) Polo, A. S.; Itokazu, M. K.; Iha, N. Y. M. Metal Complex Sensitizers in Dye-Sensitized Solar Cells. *Coord. Chem. Rev.* **2004**, *248*, 1343−1361.
(57) Sodergren, S.; Hagfeldt, A.; Olsson, J.; Lindquist, S. E. Theoretical-Models for the Action Spectrum and the Current−Voltage Characteristics of Microporous Semiconductor-Films in Photoelectrochemical Cells. *J. Phys. Chem.* **1994**, *98*, 5552−5556.
(58) Halme, J.; Boschloo, G.; Hagfeldt, A.; Lund, P. Spectral Characteristics of Light Harvesting, Electron Injection, and Steady-State Charge Collection in Pressed TiO_2 Dye Solar Cells. *J. Phys. Chem. C* **2008**, *112*, 5623−5637.
(59) Villanueva, J.; Anta, J. A.; Guillén, E.; Oskam, G. Numerical Simulation of the Current−Voltage Curve in Dye-Sensitized Solar Cells. *J. Phys. Chem. C* **2009**, *113*, 19722−19731.
(60) Chirvase, D.; Parisi, J.; Hummelen, J. C.; Dyakonov, V. Influence of Nanomorphology on the Photovoltaic Action of Polymer−Fullerene Composites. *Nanotechnology* **2004**, *15*, 1317−1323.